Comparison of Brn3a and RBPMS Labeling to Assess Retinal Ganglion Cell Loss During Aging and in a Model of Optic Neuropathy

Miranda Meng,[1] Brahim Chaqour,[1,2] Nuala O'Neill,[1] Kimberly Dine,[1,2] Neha Sarabu,[1] Gui-Shuang Ying,[1,2] Kenneth S. Shindler,[1–3] and Ahmara G. Ross[1–3]

[1]Department of Ophthalmology, University of Pennsylvania, Philadelphia, Pennsylvania, United States
[2]F. M. Kirby Center for Molecular Ophthalmology, Scheie Eye Institute, Perelman School of Medicine at the University of Pennsylvania, Philadelphia, Pennsylvania, United States
[3]Department of Neurology, University of Pennsylvania, Philadelphia, Pennsylvania, United States

Correspondence: Ahmara G. Ross, Department of Ophthalmology, University of Pennsylvania, 3500 Civic Center Boulevard, Philadelphia, PA 19104, USA; ahmara.ross@pennmedicine.upenn.edu.
Kenneth S. Shindler, F. M. Kirby Center for Molecular Ophthalmology, Scheie Eye Institute, Perelman School of Medicine at the University of Pennsylvania, 305 Stellar-Chance Laboratory, 422 Curis Blvd, Philadelphia, PA 19104, USA; kenneth.shindler@pennmedicine.upenn.edu.

Received: January 5, 2024
Accepted: March 15, 2024
Published: April 8, 2024

Citation: Meng M, Chaqour B, O'Neill N, et al. Comparison of Brn3a and RBPMS labeling to assess retinal ganglion cell loss during aging and in a model of optic neuropathy. *Invest Ophthalmol Vis Sci.* 2024;65(4):19. https://doi.org/10.1167/iovs.65.4.19

Purpose. Retinal ganglion cell (RGC) loss provides the basis for diagnosis and stage determination of many optic neuropathies, and quantification of RGC survival is a critical outcome measure in models of optic neuropathy. This study examines the accuracy of manual RGC counting using two selective markers, Brn3a and RBPMS.

Methods. Retinal flat mounts from 1- to 18-month-old C57BL/6 mice, and from mice after microbead (MB)-induced intraocular pressure (IOP) elevation, are immunostained with Brn3a and/or RBPMS antibodies. Four individuals masked to the experimental conditions manually counted labeled RGCs in three copies of five images, and inter- and intra-person reliability was evaluated by the intraclass correlation coefficient (ICC).

Results. A larger population (approximately 10% higher) of RGCs are labeled with RBPMS than Brn3a antibody up to 6 months of age, but differences decrease to approximately 1% at older ages. Both RGC-labeled populations significantly decrease with age. MB-induced IOP elevation is associated with a significant decrease of both Brn3a- and RBPMS-positive RGCs. Notably, RGC labeling with Brn3a provides more consistent cell counts than RBPMS in interpersonal (ICC = 0.87 to 0.11, respectively) and intra-personal reliability (ICC = 0.97 to 0.66, respectively).

Conclusions. Brn3a and RBPMS markers are independently capable of detecting significant decreases of RGC number with age and in response to IOP elevation despite RPBMS detecting a larger number of RGCs up to 6 months of age. Brn3a labeling is less prone to manual cell counting variability than RBPMS labeling. Overall, either marker can be used as a single marker to detect significant changes in RGC survival, each offering distinct advantages.

Keywords: retinal ganglion cells (RGCs), immunohistochemistry, RBPMS, Brn3a, optic neuropathy, manual cell count

Optic neuropathies encompass a set of neurodegenerative disorders, with notable examples including glaucoma, optic neuritis, and hereditary optic neuropathies.[1–4] RGCs, the cells most affected in optic neuropathies, are the output neurons of the vertebrate retina. Mechanistically, RGC loss and axon degeneration have been linked to activation of immune cells, altered trabecular meshwork cells, neuroinflammatory processes, dysregulated gut microbiota, and oxidative stress.[5–7]

Identifying disease-specific kinetics and patterns of RGC loss is central to understanding the pathophysiology of neurodegenerative diseases, with important contributions made in mouse models of optic neuropathies. Whereas visualization in vivo with developing methods has contributed to some progress in qualitative and quantitative analyses of RGC loss,[8,9] standard quantification commonly relies on immunohistochemical analyses of histological preparations of the retina using molecular markers of RGCs.[10–12] Therefore, use of specific RGC markers is necessary for accurate qualitative and quantitative analyses of cell loss in animal models of optic neuropathies and to evaluate the efficacy of relevant treatment approaches.

The Brn3a/Pou4f1 transcription factor is selectively expressed by cells in the ganglion cell layer, a pattern maintained in healthy and injured retinas.[13] Brn3a is also a nuclear label, making Brn3a staining clear and well delineated.[11] However, previous studies have suggested that Brn3a was expressed in only 80% of RGCs[14] labeled with another commonly used marker, RNA binding protein with multiple splicing (RBPMS) protein.[15] Thus, retinal labeling with Brn3a may result in an underestimation of the total number of RGCs in mice. Whether Brn3a labels a high enough percentage of RGCs to identify differences in their

loss or lack thereof in different experimental and physiologic conditions is not fully understood.

The present study was designed to address the relative suitability of Brn3a and RBPMS as markers of RGCs during aging and in induced RGC loss. Studies were designed to compare the ability of each marker to identify significant age- or disease-related changes in RGC numbers, and assess the consistency of manual cell counts performed with each marker. For this purpose, retinas from (1) aging wild-type mice, and (2) mice undergoing microbead (MB)-induced ocular hypertension were used to analyze the expression of Brn3a and RBPMS protein.

Materials and Methods

Animals

The C57BL/6J mice were obtained from the Jackson Laboratory and raised in a 12-hour light/dark cycle. Animals were housed at the University of Pennsylvania animal facility in compliance with the ARVO Statement for the Use of Animals in Ophthalmic and Vision Research, IACUC, and federal regulations.

Microbead-Induced Ocular Hypertension

Ocular hypertension was induced as described previously.[16] Briefly, mice received injections of 1.5 µL of magnetic microbeads (1.6×10^6 beads/µL saline) in the anterior chamber of the right eye and concurrent injections of balanced salt solution (BSS) in the left eye. IOP was measured in the eye immediately before the first injection, and then weekly with the Icare TONOLAB tonometer (Icare TONOVET, Vantaa, Finland) in awake, unanesthetized animals.

Wholemount Immunofluorescent Staining and RGC Quantification

RGC staining and quantification was performed as previously described.[11,16–18] Mice were euthanized by cervical dislocation, and their eyes were fixed in 4% paraformaldehyde solution for 1 hour at room temperature. Following extraction of the entire retina from the optic cups, the tissues were then permeabilized in 0.5% Triton X-100 in PBS and freezing in −80°C for 15 minutes. Retinas were blocked in a blocking solution of 2% Triton X-100 (Fisher Scientific; Cat# BP151-100), 2% normal bovine serum albumin (Sigma-Aldrich, St. Louis, MO, USA; Cat# A2153-10G), and PBS for 30 minutes. Samples were incubated with a primary antibody solution containing guinea pig polyclonal anti-RBPMS antibody (Sigma-Aldrich, Darmstadt, Germany; Cat# ABN1376, 1:200) and/or rabbit polyclonal anti-Brn3a antibody (Synaptic Systems, Goettingen, Germany; Cat# 411 003, 1:1000) overnight at 4°C. Retinas were washed with PBS 6 times, then incubated in a secondary antibody solution of 1:500 goat anti-guinea pig Cy3 antibody (Abcam; Cat# ab102370) and/or 1:1000 donkey anti-rabbit AlexaFluor 488 (Invitrogen, Rockford, IL, USA; Cat# A32790) antibody for 1 hour. Retinas were flattened and mounted, vitreous side upward, with Fluoromount G mounting medium (Southern Biotech, Birmingham, AL, USA; Cat# 0100-01). After masking photographers to the experimental cohorts, the photographs were taken using a fluorescence microscope and Nikon NIS-Elements Imaging Software at 40 times magnification in 12 standard fields per retina: 1/6, 3/6, and 5/6 of the retinal radius from the center in each quadrant. The 12 fields covered a total area of 0.407 mm^2/retina. Human counters quantified RBPMS+ and Brn3a+; RBPMS+ and Brn3a-; and RBPMS- and Brn3a+ RGCs in the 12 representative fields using ImageJ software. RGC counts across the 12 representative fields were totaled for comparisons between markers.

Assessment of Interpersonal and Intrapersonal Reliability of Human Counters

Representative images were selected from whole mount retinas stained with either Brn3a or RBPMS to represent the level of clarity and brightness typical of RGCs stained with either marker. Five representative images were taken from separate retinas in central retinal fields with a high density of RGCs, for both Brn3a and RBPMS. Each selected representative image was mirrored along both the vertical and horizontal midline, generating three copies of each image. All images (3 mirrored copies × 5 images/marker × 2 markers = 30 total images) were sorted into a random order without placing two mirrored copies of the same image next to each other. All images were colorized in red, and were manually counted on ImageJ by four individuals masked to the staining conditions.

Statistical Analyses

Data were presented as the mean ± SD. RGC counts were compared using an unpaired two-tailed student's *t*-test. For multiple group analyses, statistical significance was determined using the Mann–Whitney *U* test, 1-way ANOVA, or ANOVA of repeated measures followed by Tukey's honest significant difference test, as indicted in each figure legend. Welch's correction was used when sample sizes differed. Normality of data were checked using the Kolmogorov-Smirnov test, with Dallal-Wilkinson-Lillie for corrected *P* value. Analysis of interpersonal and intrapersonal reliability for counting RGCs was performed using the intraclass correlation coefficient (ICC). The two-way random effects model with absolute agreement and single rater/measurement model was used for calculating ICC and its 95% confidence interval (95% CI).[19] Reliability was considered "poor" at ICC < 0.50, "moderate" at ICC ≥ 0.50, "good" at ICC ≥ 0.75, and "excellent" at ICC ≥ 0.90. GraphPad Prism 5.0 (GraphPad Software, Inc., La Jolla, CA, USA) was used for all statistical comparisons.

Results

Brn3a and RBPMS Immunostaining Shows Both Markers Identify RGC Loss During Aging

We determined and contrasted the expression pattern of Brn3a and RBPMS in mouse retina at different stages of postnatal life. Retinas were harvested from 1- to 18-month-old mice, immunolabeled with Brn3a and RBPMS antibodies, and imaged by fluorescence microscopy. Representative images of Brn3a- and RBPMS-labeled and merged Brn3a- and RBPMS-positive cells are shown in Figure 1A. Immunolabeled cells were counted by masked investigators. Both Brna3a-positive (Fig. 1B) and RPBMS-positive (Fig. 1C) cells showed similar significant decreases in cell counts with aging. Co-immunostaining of 1- and 6-month-old mouse retinas with RBPMS and Brn3a showed that 99.95 ± 0.02% and 99.64 ± 0.14% of all Brn3a-positive RGCs were also

Investigative Ophthalmology & Visual Science

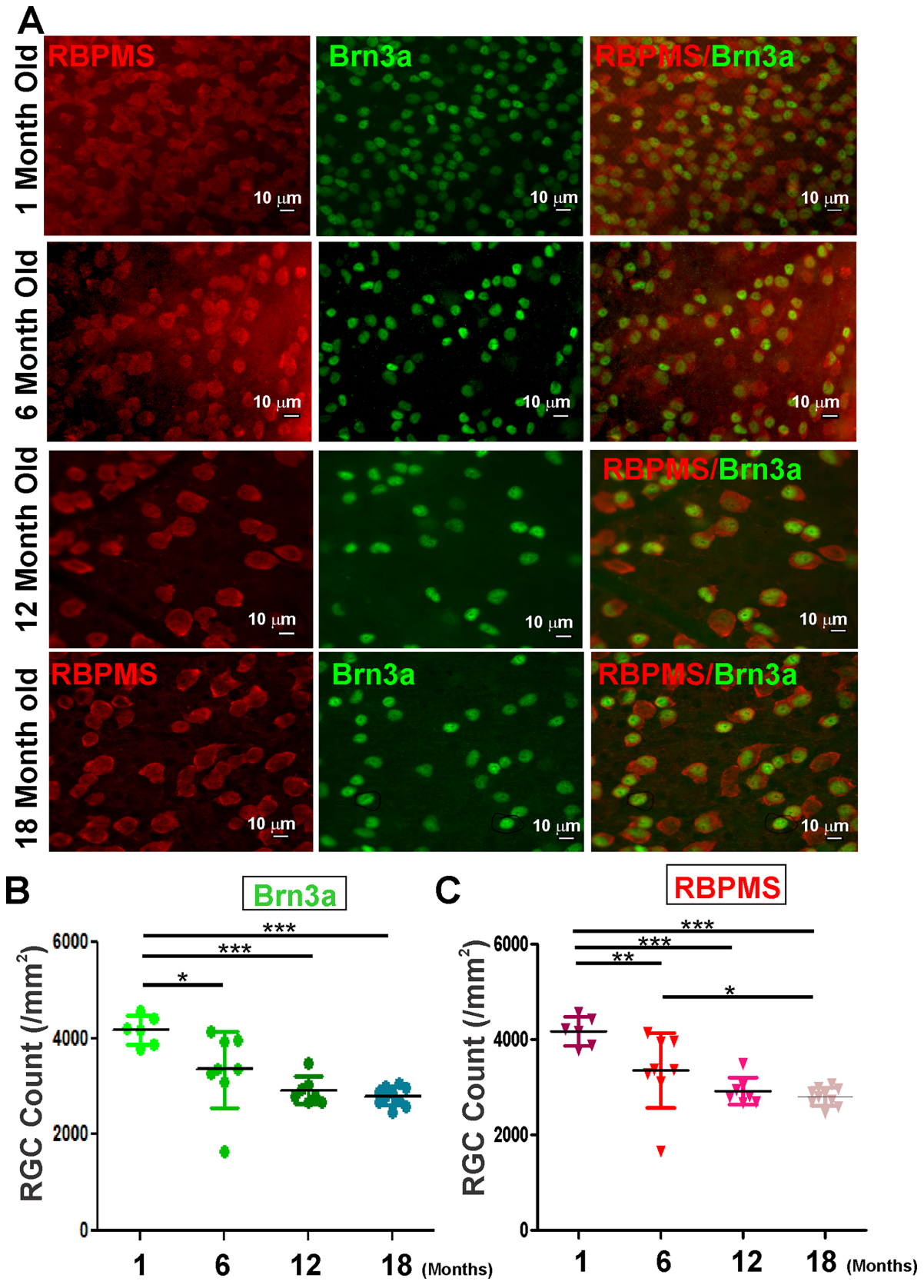

Figure 1. Effects of aging on RGC marker expression. (**A**) Representative fluorescence micrographs of flat mounted wild-type mouse retina co-stained with antibodies against Brn3a and RBPMS markers of RGCs. Displayed images were taken half of the retinal radius from the center of the retina at 1, 6, 12, and 18 months of age. (**B, C**) The number of Brn3a (**B**) and RPBMS (**C**) labeled RGCs per sampled retinal area at different postnatal stages is shown. An average of all retinal fields quantified (central, mid-peripheral, and peripheral) are shown as mean ± standard deviation (n = 6–10). Significance was determined by 1-way ANOVA and Tukey's multiple comparisons test. * $P < 0.05$, ** $P < 0.01$, *** $P < 0.001$.

Investigative Ophthalmology & Visual Science

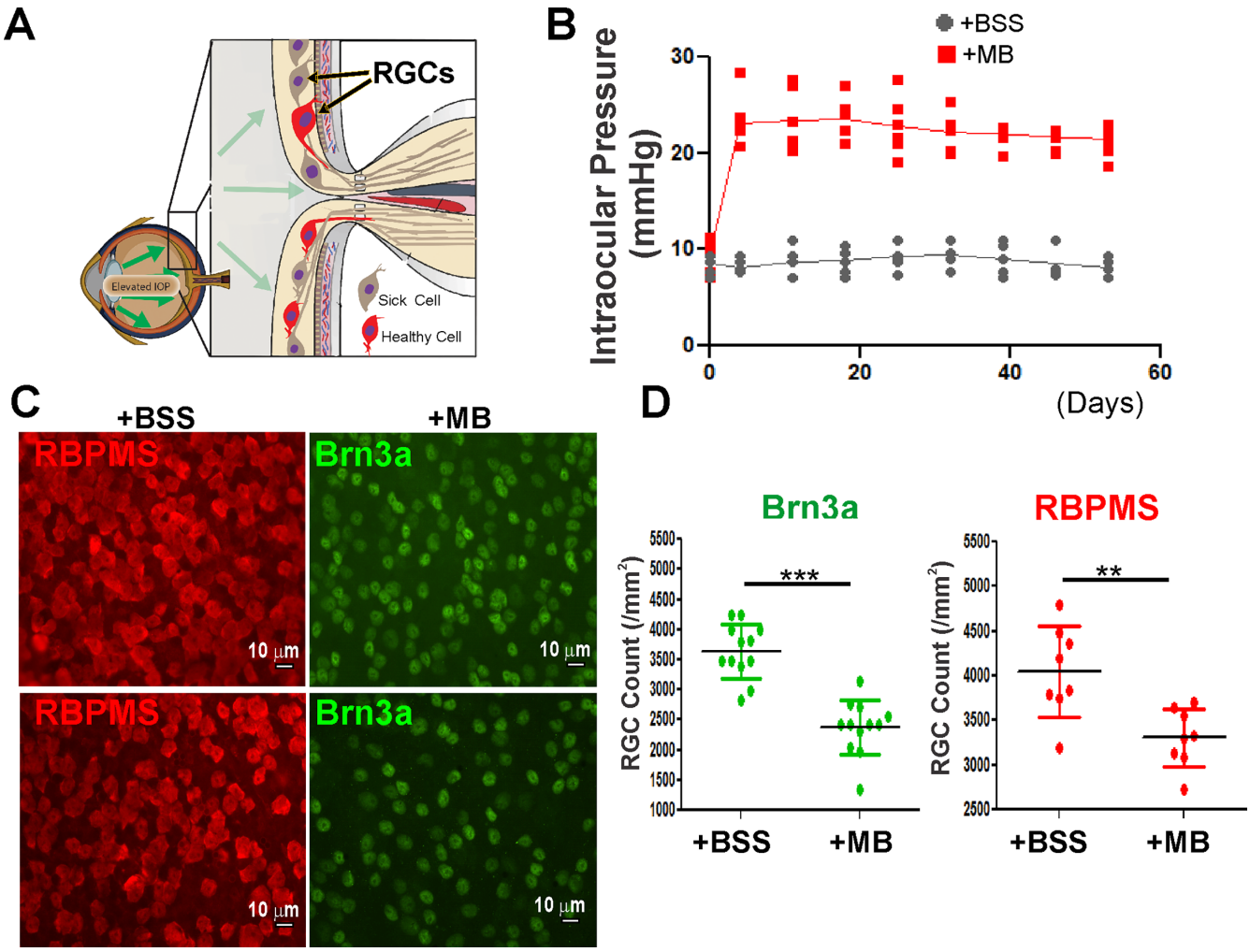

Figure 2. Effects of MB-induced IOP elevation on RGC marker expression. (**A**) Mice were injected in the anterior chamber with MBs in one eye and BSS in the contralateral eye. (**B**) IOP was elevated in the MB-injected compared to the BSS-injected eyes. (**C**) Representative Brn3a- and RBPMS- immunofluorescently labeled flat mounted mouse retinas sampled from the mid-peripheral retina from BSS- and MB-injected mouse eyes taken at 40 times magnification. (**D**) Total number of Brn3a- and RBPMS-labeled RGCs per area in the control BSS-injected and MB-injected mouse eyes. An average of all retinal fields quantified (central, mid-peripheral, and peripheral) are shown as means ± standard deviation (n = 8–12). Data represented as mean ± SEM. ** $P < 0.01$ and *** $P < 0.001$ by an unpaired one-sided t-test.

RBPMS-positive, respectively (see Figs. 1B, 1C). However, approximately 9.77% and 6.44% of all RBPMS-positive cells were Brn3a-negative in 1- and 6-month-old mouse retinas, respectively. At 1 month of age, RBPMS-positive RGC counts were 9.78 ± 2.9% higher than Brn3a-positive RGC counts. At 6 months, RBPMS still stained a greater number or RGCs than Brn3a. However, at 12 and 18 months of age, the numbers of Brn3a-positive cells were not significantly higher than those of RBPMS-positive cells.

Brn3a and RBPMS Markers Both Support Detection of Significant RGC Loss in the MB-Induced IOP Elevation Model

We used the MB-induced ocular hypertension model to contrast the effects of high IOP on Brn3a- and RBPMS-positive cells in mouse retinas (Fig. 2A). MB injection resulted in an increase in IOP which remained elevated throughout the time course of the experiment as compared to baseline before MB injection (Fig. 2B). IOP did not increase in control eyes of BSS-injected mice.

Retinal flat mounts were prepared from BSS- and MB-injected mouse eyes and immunolabeled with Brn3a and RBPMS antibodies (Fig. 2C), and labeled cells were counted. There was a significant decrease in the number of both RBPMS- and Brn3a-positive cells in the MB-injected mouse group compared to their respective control group (Fig. 2D).

Reliability of Manual Counting of Brn3a- and RBPMS-Positive RGCs by the Same and Different Counters

Any study relying on manual counting of hundreds of cells in retinal flat mount images are prone to errors and reproducibility issues due to human biases/errors that can be linked to variable training, experience, subjectivity, recognition bias, and fatigue. Staining intensity and background illumination of immunostained retinas could further increase

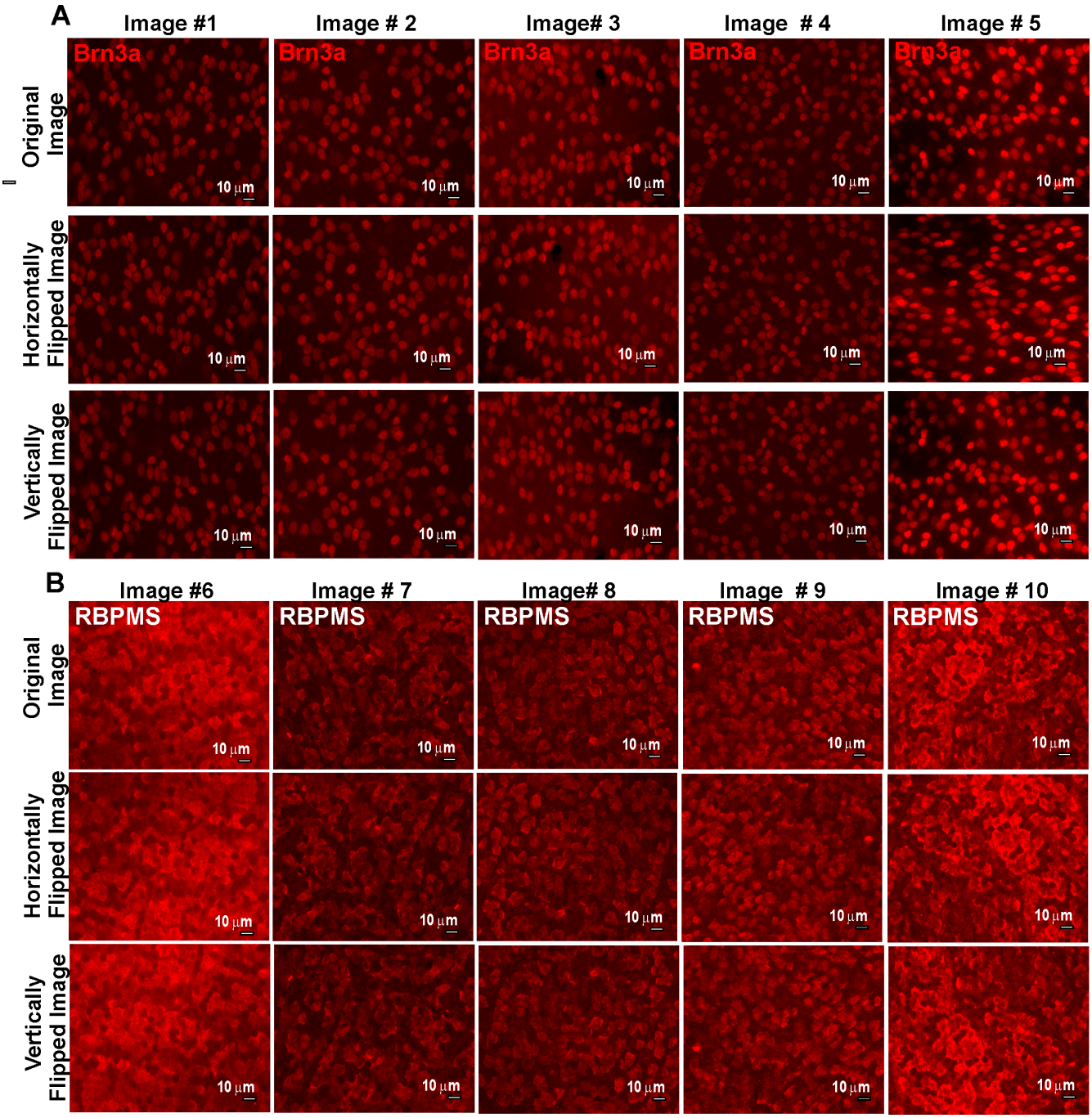

Figure 3. Retinal images used to assess variability of manual counts. Retinal flat mount from wild-type mice stained with either Brn3a (**A**) or RBPMS (**B**) antibodies**.** Each original image was duplicated and flipped either horizontally (*middle row*) or vertically (*bottom row*). This change of the orientation of the images was performed to determine the reliability of the cell count of the same image by individual counters who did not know that the same images were being counted in different orientations.

subjectivity of cell counting by users/counters. To assess the reliability of cell counts by the same and different individual counters (i.e. masked individual investigators), five images of Brn3a- and RBPMS-stained sections of retinal flat mounts were presented to four individuals for counting (Fig. 3). Three copies of each image: one original, one flipped horizontally, and one flipped vertically, were included in the image pool distributed to each person for counting. Individual cell counts obtained from every investigator on all copies of each image are listed in the Table. Figures 4A and 4B show that changing the orientation of the image (flipped horizontally or vertically) did not significantly affect the cell counts averaged across all 4 counters, as compared to the original image, whether RGCs were Brn3a- or RBPMS-labeled. We further performed analyses to assess the degree of intrapersonal and interpersonal reliability of manual counts of

Investigative Ophthalmology & Visual Science

Table. Individual Cell Counts From Four Masked Investigators

	Counter 1	Counter 2	Counter 3	Counter 4
Brn3a-Labeled Cells				
Retinal image 1				
Original	184	174	186	186
Vertically flipped	181	176	187	184
Horizontally flipped	182	176	186	186
Retinal image 2				
Original	154	151	158	161
Vertically flipped	150	151	155	162
Horizontally flipped	154	147	157	165
Retinal image 3				
Original	196	189	221	208
Vertically flipped	193	195	208	216
Horizontally flipped	200	191	204	203
Retinal image 4				
Original	175	171	177	177
Vertically flipped	172	170	178	181
Horizontally flipped	173	169	181	179
Retinal image 5				
Original	160	154	171	172
Vertically flipped	160	154	168	161
Horizontally flipped	157	152	166	169
RBPMS-Labeled Cells				
Retinal image 6				
Original	122	195	191	236
Vertically flipped	112	211	167	239
Horizontally flipped	142	228	174	216
Retinal image 7				
Original	152	182	189	221
Vertically flipped	144	203	168	226
Horizontally flipped	164	169	196	226
Retinal image 8				
Original	162	202	183	227
Vertically flipped	160	188	191	210
Horizontally flipped	154	202	190	226
Retinal image 9				
Original	176	215	226	268
Vertically flipped	176	203	209	257
Horizontally flipped	177	227	229	259
Retinal image 10				
Original	163	197	186	198
Vertically flipped	162	188	196	220
Horizontally flipped	150	205	180	214

RGCs labels with each marker. The standard deviations of the cell counts of the three copies of each image performed by each individual counter were significantly higher for RBPMS-labeled cells as compared with Brn3a-labeled cells (Figs. 5A–D). We also determined the ICC as an indicator of the consistency of cell counts made by individual cell counters counting three copies of the same images (intrapersonal variability), and the consistency of four different cell counters counting the same image (interpersonal variability). Figures 5E and 5F show ICC analysis of images stained with Brn3a detected very good interpersonal reliability (ICC = 0.866, 95% CI = 0.7894–0.9429) and excellent intrapersonal reliability (ICC = 0.970, 95% CI = 0.9401–0.9995). However, images stained with RBPMS antibodies had poor interpersonal reliability (ICC = 0.110, 95% CI = −0.027 to 0.2479) and only moderate intrapersonal reliability (ICC = 0.657, 95% CI = 0.3141–0.9995). These results suggest that there is greater variability in reliability for counting of RBPMS-labeled cells compared to that of Brn3a-labeled cells.

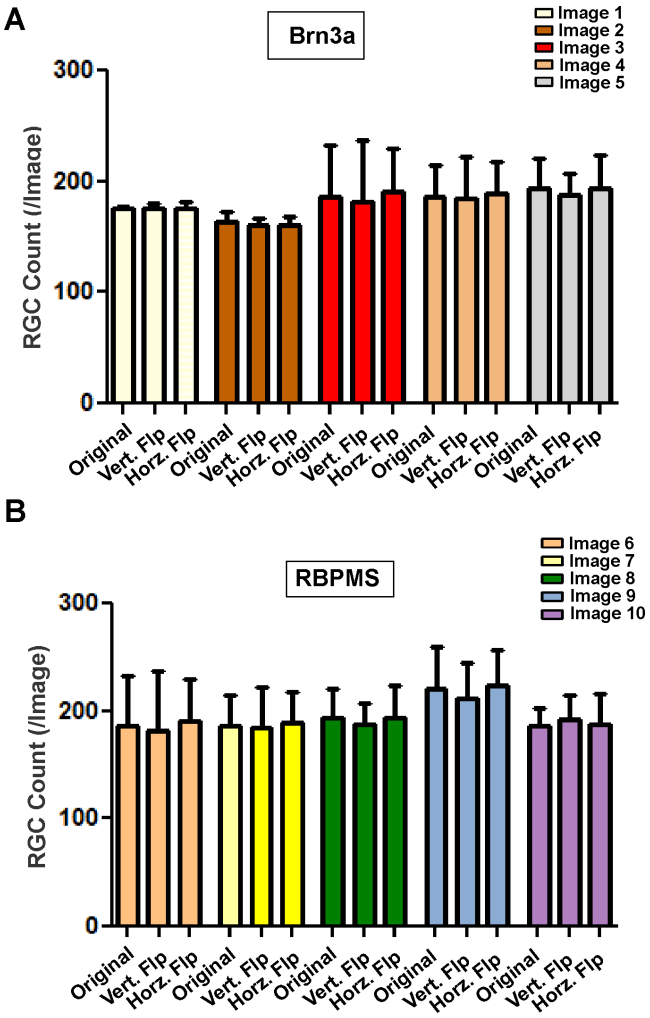

Figure 4. Average RGC counts show masked investigators are fairly consistent in identifying both Brn3a- and RPBMS-positive RGCs. Graphs show the average (mean ± standard deviation) number of (**A**) Brn3a- and (**B**) RBPMS-positive cell counts in retinal flat mount images. RGC count in an image is compared to those of the same image oriented horizontally or vertically by counters masked to the orientation changes ($n = 4$ counters/image). For each image, there is no significant difference between the number of RGCs counted in the original orientations versus either flipped orientation. Standard deviations show there is modest variability of RGC counts between individual counters in all five RPBMS labeled images, but only three of five Brn3a labeled images.

Discussion

RGC immunolabeling with neuronal markers, such as Brn3a, RBPMS, b III-tubulin, or g-synuclein, and manual counting of the labeled RGCs in images, are commonly used methods to evaluate RGC loss in animal models of RGC degeneration and after implementation of experimental therapies.[12] Brn3a along with Brn3b and Brn3c are highly expressed in postmitotic RGCs.[20] Brn3a (alone or with Brn3b/c) is expressed in 96% of RGCs whereas the remaining 4% express Brn3b alone.[21] Interestingly, loss of function of Brn3a did not lead to a retinal phenotype.[22] However, replacement of the Brn3b gene by the Brn3a coding sequence prevented RGC loss in Brn3b knockout mice suggesting that Brn3a and Brn3b are functionally redundant in RGCs.[23] Studies have shown that Brn3b plays a role in RGC axon development,

Investigative Ophthalmology & Visual Science

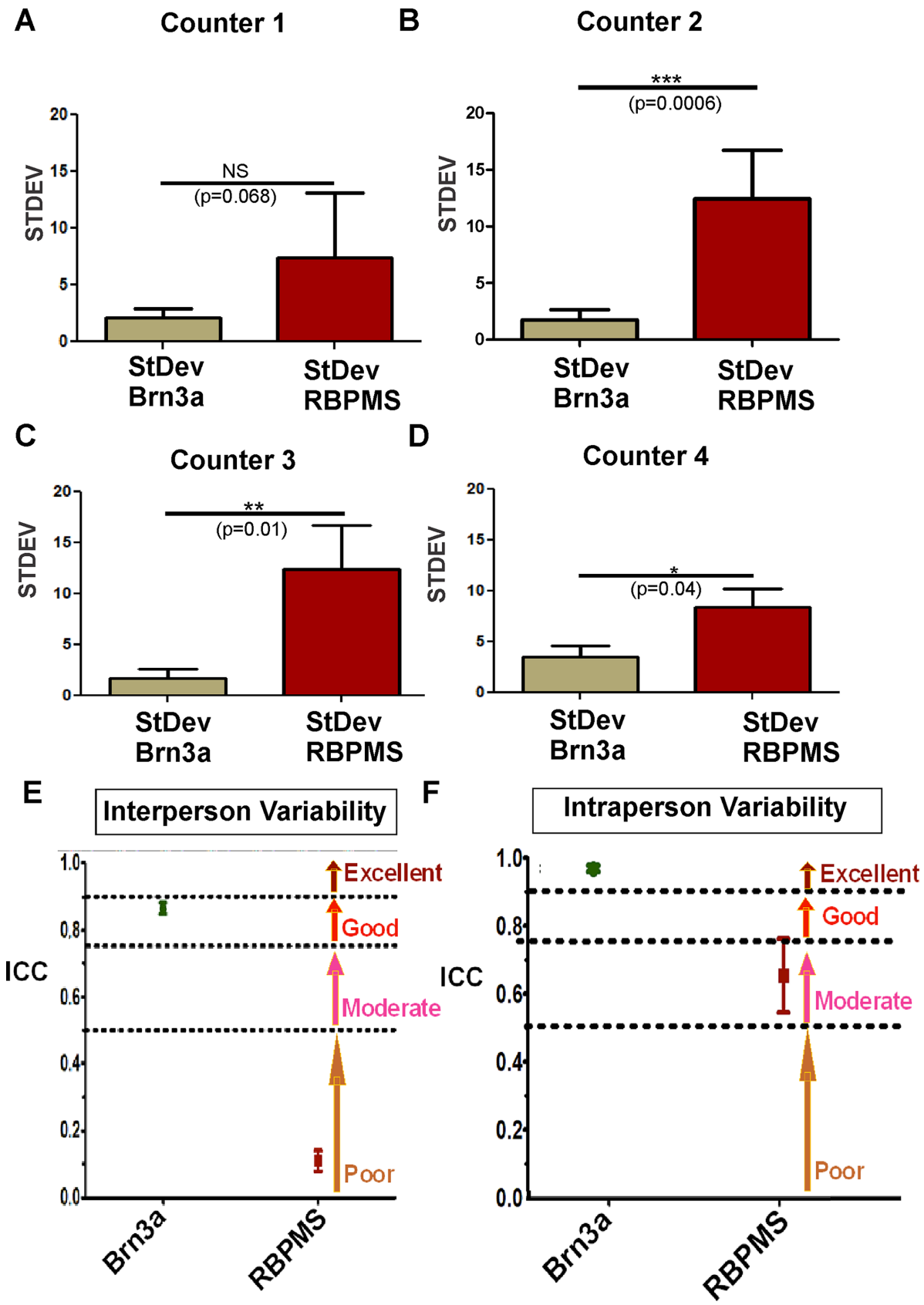

Figure 5. Quantitative analysis of interpersonal and intrapersonal variability of manual counting of Brn3a and RBPMS-labeled RGC. (**A–D**) The standard deviation of RGC counts was calculated for counts of the three different orientations of each individual image obtained from each masked investigator, in order to assess differences in intrapersonal quantification of RGCs labeled with different cell markers. Graphs show the average standard deviations of Brn3a and RBPMS-positive cell counts (n = 5 images/counter for each RGC marker).

Investigative Ophthalmology & Visual Science

Standard deviations were significantly higher for RBPMS-labeled images as compared with the standard deviation of Brn3a cell counts from three of four investigators (**B–D**), with a similar strong trend seen with counter 1 (**A**). Data represented as mean ± standard deviation ($n = 5$); comparisons by unpaired student's *t*-test. (**E, F**) The relative reliability of both interpersonal (**E**) and intrapersonal (**F**) cell counts was further analyzed for both Brn3a (*green bars*) and RPBMS (*red bars*) labeled cells using the intraclass correlation coefficient (ICC). Lines indicate cutoffs for "poor" (<0.50), "moderate" (≥0.50), "good" (≥0.75), and "excellent" (≥0.90) reliability between counts. ICC shows that there is very good interpersonal reliability and excellent intrapersonal reliability of manual counts of Brn3a-positive cells; whereas, there is poor interpersonal reliability and only moderate intrapersonal reliability of manual counts of RPBMS-positive cells. Data represented as mean ± SEM.

whereas Brn3a is involved in differentiation of dendritic arbors.[24] Thus, loss of Brn3a expression can be equated with either RGC loss or dysfunction. For the RBPMS marker, this is an important regulator of mRNA processing, trafficking, cellular location, and translation of their target mRNAs.[25] RGCs express high levels of RBPMS and its transcripts have been used extensively as markers of this cell population.

In this study, we evaluated the relative accuracy of RGC labeling with Brn3a and RBPMS, and assessed potential variability between counters. Microscope images of labeled RGCs demonstrated different and distinct advantages of RGC labeling with either Brn3a or RBPMS staining. Brn3a nuclear staining provided well resolved fluorescence signals making it subjectively easier to identify and reliably count them. This subjective reliability was supported quantitatively by lower standard deviations between identical images of Brn3a-labeled cells counted by individual investigators, as well as smaller ICC for interpersonal and intrapersonal reliability of RGC counts as compared with RPBMS-labeled cells. In contrast, immunolabeling with RBPMS was detectable in the cytoplasm, consistent with its role in posttranscriptional regulation of gene expression, including mRNA translation, processing, transport, and stability.[26] RBPMS immunostaining of RGCs often showed cells clustered together, overlapping one another with undefined boundaries, thus making them subjectively more difficult to count accurately, particularly in regions with higher cell density.[14] The higher reliability observed here suggests that Brn3a may offer some advantages as a RGC marker. Nonetheless, because of their layering, a few Brn3a-positive RGCs appeared blurred in the images, highlighting that distinguishing and counting a small subset of RGCs may be limited regardless of the marker used.

Of note, our data also showed that RPBMS labeled a higher percentage of RGCs than Brn3a, up to 6 months of age. We found that nearly 10% of RBPMS-positive cells were Brn3a-negative. This is consistent with previous studies by Rodriguez et al. showing that RBPMS is expressed by nearly the entire RGC population in different mammalian species.[14] Indeed, a greater number of RGCs were found to be retrogradely labeled by fluorescent dyes than the number of Brn3a-immunolabeled RGCs.[27] This could be of significance particularly in neurodegenerative diseases wherein some subpopulations of RGCs could be more affected than others. Indeed, Sanes and Marshal have estimated that there are likely more than 30 different subtypes of RGCs and each RGC subtype projects to multiple targets in the central nervous system.[28,29] These findings suggest some advantage of RBPMS as a marker of RGCs versus Brn3a. In experiments estimating RGC numbers across the entire mouse retina, it has been determined that Brn3a staining may miss about 2000 to 6000 RGCs, because the total number of RGCs in C57BL/6 mouse retina has been estimated to be between 40,000 and 60,000 cells.[30] Whether or not this affects the ability of an experiment to detect significant changes will ultimately depend on the goal of each study.

In addition to these experimentally inherent extraneous variables, cell counting errors associated with subjective bias of counters/users add another layer of uncertainty to the accuracy of RGC counts. Manual counting using ImageJ is a laborious, time-consuming process prone to errors.[31] When we compared counting results of the same slides by different individuals, we found that RBPMS-positive cell counting was associated with poorer interpersonal and intrapersonal reliability than Brn3a among different masked counters. Brn3a had good reliability, but RBPMS showed poor reliability (ICC <0.50). This suggests that, if multiple users perform RGC counting in the same study, significant variations may be observed among them, and this could confound the counting results. Poor-quality retinal images, including low-contrast RGC fluorescence and high-density RGCs, could further exacerbate subjective bias of manual counting.

Accurate counting of the number of RGCs and an appropriate representative RGC population is critical when evaluating the extent of retinal neurodegeneration in physiologic aging, in optic neuropathies, and after experimental manipulation. Our data showed that aging caused a significant decrease of the number of both Brn3a- and RBPMS-positive RGCs in 6-month-old mice and beyond when compared to 1 month old mice. Similar statistically significant declines in cell numbers were detected in retinas stained with either Brn3a or RPBMS even with the use of relatively modest numbers of animals in each age group, suggesting that immunolabeling with either Brn3a or RBPMS allowed visualization of a sufficient number of RGCs to reveal the age-related changes despite counting errors inherent to the use of these markers as well as any potential subjective counter bias. The significant decrease in the percent of Brn3a-negative RBPMS-positive RGCs we observed from 1 to 6 months of age (from 9.77% at 1 month to 6.44% at 6 months), is consistent with prior studies by Boehme et al. who showed that 8.9% of Brn3a-negative RBPMS-positive RGCs were observed in 13 to 17-week-old mice.[32] After 6 months of age, we found no significant change in the percent of RBPMS- and Brn3a-positive RGCs, as RBPMS antibodies consistently stained RGCs that Brn3a antibodies did label, in agreement with previous studies.[14] The decrease in the percent of Brn3a-negative RBPMS-positive cells could be due to changes in protein degradation leading up to 6 months of age, or that RBPMS-positive and Brn3a-negative RGCs tend to die first with age. Further investigation of the time course of Brn3a and RBPMS protein turnover and breakdown are needed to examine how aging affects RGC survival.

In the ocular hypertension model of MB-induced IOP elevation, there was a significant decrease in both Brn3a-positive and RBPMS-positive RGC counts, in mice injected with MBs. There was a trend toward greater loss of Brn3a-positive RGCs (>30% decrease) compared to RBPMS-

Investigative Ophthalmology & Visual Science

positive cells (approximately 18%), which may suggest selective decrease in Brn3a protein expression in the MB model of neurodegeneration. However, results showed that both markers were able to detect significant RGC loss even in using a modest number of animals, suggesting that either marker may be useful for future neuroprotective studies where the goal is to determine whether treatments reduce the amount of RGC loss.

Overall, our study provides valuable information about the reliability of manual counting of RGCs labeled with either Brn3a or RBPMS within representative retinal fields. Although there is potential for sampling bias, this is partially reduced by use of masked investigators. Various algorithms have also been developed to perform automatic counting of RGCs, although some may still require manually adjusting some parameters.[10,30] Whereas preferred in many experiments, particularly where staining is ideal, it is also recognized that often in diseased retinas or other situations where staining is less clear, automated counting may introduce more variability than manual counting.[11] Thus, by design, the current studies evaluated staining in a commonly used manual counting method. The potential applicability of the current findings to automated RGC counting remains to be examined.

In conclusion, accurate identification and quantification of RGCs is important for experimental studies examining physiologic changes, as well as ocular neurodegeneration and neuroprotection. RBPMS is a valuable marker as it labels nearly the entire population of RGCs, but results suggest counting RBPMS-positive cells may be prone to small yet significant errors. In contrast, Brn3a labeling yielded fewer counting errors, although it did not stain the entire RGC population. The use of both markers can reveal significant changes in RGC loss or survival in disease models of neuronal degeneration, but current results demonstrate that either marker alone provides a useful method to detect significant RGC loss due to aging or elevated IOP, and suggests that potential advantages exist for each of these two markers when investigators select a marker to use in optic neuropathy models. Specifically, we found that Brn3a offers qualitative and quantitative advantages in the reliability of immunohistochemical labeling and manual counting of RGCs, and Brn3a staining can provide statistically valuable information reflecting retinal neurodegeneration or lack thereof when used as a single marker, even though RPBMS serves as a more widespread marker present in nearly all RGC subpopulations.

Acknowledgments

The authors thank Jacob Rossman for assistance as a masked counter of RBPMS and Brn3a-positive cells, and we also thank Jipeng Yue for technical support with immunohistochemistry, and with photographing and counting cells.

Supported by the National Institutes of Health Grants (EY019014, EY301163, and P30EY01583), RWJ-Harold Amos Faculty Development Award, Linda Pechenik Montague Investigator Award, Dean's Innovation Fund, Research to Prevent Blindness, Paul and Evanina Mackall Foundation Trust, Center for Advanced Retinal and Ocular Therapeutics, and the F. M. Kirby Foundation.

Disclosure: **M. Meng**, None; **B. Chaqour**, None; **N. O'Neill**, None; **K. Dine**, None; **N. Sarabu**, None; **G.-S. Ying**, None; **K.S. Shindler**, None; **A.G. Ross**, None

References

1. Wu GF, Parker Harp CR, Shindler KS. Optic neuritis: a model for the immuno-pathogenesis of central nervous system inflammatory demyelinating diseases. *Curr Immunol Rev*. 2015;11:85–92.
2. Newman NJ, Yu-Wai-Man P, Biousse V, Carelli V. Understanding the molecular basis and pathogenesis of hereditary optic neuropathies: towards improved diagnosis and management. *Lancet Neurol*. 2023;22:172–188.
3. Chapelle AC, Rakic JM, Plant GT. The occurrence of intraretinal and subretinal fluid in anterior ischemic optic neuropathy: pathogenesis, prognosis, and treatment. *Ophthalmology*. 2023;130:1191–1200.
4. Soucy JR, Aguzzi EA, Cho J, et al. Retinal ganglion cell repopulation for vision restoration in optic neuropathy: a roadmap from the RReSTORe Consortium. *Mol Neurodegener*. 2023;18:64.
5. Kang EY, Liu PK, Wen YT, et al. Role of oxidative stress in ocular diseases associated with retinal ganglion cells degeneration. *Antioxidants (Basel)*. 2021;10.
6. Sanz-Morello B, Ahmadi H, Vohra R, et al. Oxidative stress in optic neuropathies. *Antioxidants (Basel)*. 2021;10.
7. Wong KA, Benowitz LI. Retinal ganglion cell survival and axon regeneration after optic nerve injury: role of inflammation and other factors. *Int J Mol Sci*. 2022;23:10179.
8. Ito A, Tsuda S, Kunikata H, Toshifumi A, Sato K, Nakazawa T. Assessing retinal ganglion cell death and neuroprotective agents using real time imaging. *Brain Res*. 2019;1714:65–72.
9. Balendra SI, Normando EM, Bloom PA, Cordeiro MF. Advances in retinal ganglion cell imaging. *Eye (Lond)*. 2015;29:1260–1269.
10. Geeraerts E, Dekeyster E, Gaublomme D, Salinas-Navarro M, De Groef L, Moons L. A freely available semi-automated method for quantifying retinal ganglion cells in entire retinal flatmounts. *Exp Eye Res*. 2016;147:105–113.
11. Shindler RE, Yue J, Chaqour B, Shindler KS, Ross AG. Repeat Brn3a immunolabeling rescues faded staining and improves detection of retinal ganglion cells. *Exp Eye Res*. 2023;226:109310.
12. Miralles de Imperial-Ollero JA, Vidal-Villegas B, Gallego-Ortega A, et al. Methods to identify rat and mouse retinal ganglion cells in retinal flat-mounts. *Methods Mol Biol*. 2023;2708:175–194.
13. Latchman DS. The Brn-3a transcription factor. *Int J Biochem Cell Biol*. 1998;30:1153–1157.
14. Rodriguez AR, de Sevilla Muller LP, Brecha NC. The RNA binding protein RBPMS is a selective marker of ganglion cells in the mammalian retina. *J Comp Neurol*. 2014;522:1411–1443.
15. Kwong JM, Caprioli J, Piri N. RNA binding protein with multiple splicing: a new marker for retinal ganglion cells. *Invest Ophthalmol Vis Sci*. 2010;51:1052–1058.
16. Yue J, Khan RS, Duong TT, et al. Cell-specific expression of human SIRT1 by gene therapy reduces retinal ganglion cell loss induced by elevated intraocular pressure. *Neurotherapeutics*. 2023;20:896–907.
17. Khan RS, Baumann B, Dine K, et al. Dexras1 deletion and iron chelation promote neuroprotection in experimental optic neuritis. *Sci Rep*. 2019;9:11664.
18. Ross AG, Chaqour B, McDougald DS, et al. Selective upregulation of SIRT1 expression in retinal ganglion cells by AAV-mediated gene delivery increases neuronal cell survival and alleviates axon demyelination associated with optic neuritis. *Biomolecules*. 2022;12:830.
19. Koo TK, Li MY. A guideline of selecting and reporting intraclass correlation coefficients for reliability research. *J Chiropr Med*. 2016;15:155–163.

Investigative Ophthalmology & Visual Science

20. Latchman DS. Activation and repression of gene expression by POU family transcription factors. *Philos Trans R Soc Lond B Biol Sci*. 1996;351:511–515.
21. Nadal-Nicolas FM, Jimenez-Lopez M, Salinas-Navarro M, et al. Whole number, distribution and co-expression of brn3 transcription factors in retinal ganglion cells of adult albino and pigmented rats. *PLoS One*. 2012;7:e49830.
22. Quina LA, Pak W, Lanier J, et al. Brn3a-expressing retinal ganglion cells project specifically to thalamocortical and collicular visual pathways. *J Neurosci*. 2005;25:11595–11604.
23. Pan L, Yang Z, Feng L, Gan L. Functional equivalence of Brn3 POU-domain transcription factors in mouse retinal neurogenesis. *Development*. 2005;132:703–712.
24. Badea TC, Cahill H, Ecker J, Hattar S, Nathans J. Distinct roles of transcription factors brn3a and brn3b in controlling the development, morphology, and function of retinal ganglion cells. *Neuron*. 2009;61:852–864.
25. Lunde BM, Moore C, Varani G. RNA-binding proteins: modular design for efficient function. *Nat Rev Mol Cell Biol*. 2007;8:479–490.
26. Yang Y, Lee GC, Nakagaki-Silva E, et al. Cell-type specific regulator RBPMS switches alternative splicing via higher-order oligomerization and heterotypic interactions with other splicing regulators. *Nucleic Acids Res*. 2023;51:9961–9982.
27. Galindo-Romero C, Aviles-Trigueros M, Jimenez-Lopez M, et al. Axotomy-induced retinal ganglion cell death in adult mice: quantitative and topographic time course analyses. *Exp Eye Res*. 2011;92:377–387.
28. Duan X, Qiao M, Bei F, Kim IJ, He Z, Sanes JR. Subtype-specific regeneration of retinal ganglion cells following axotomy: effects of osteopontin and mTOR signaling. *Neuron*. 2015;85:1244–1256.
29. Sanes JR, Masland RH. The types of retinal ganglion cells: current status and implications for neuronal classification. *Annu Rev Neurosci*. 2015;38:221–246.
30. Claes M, Moons L. Retinal ganglion cells: global number, density and vulnerability to glaucomatous injury in common laboratory mice. *Cells*. 2022;11:2689.
31. Maidana DE, Tsoka P, Tian B, et al. A novel ImageJ macro for automated cell death quantitation in the retina. *Invest Ophthalmol Vis Sci*. 2015;56:6701–6708.
32. Boehme NA, Hedberg-Buenz A, Tatro N, et al. Axonopathy precedes cell death in ocular damage mediated by blast exposure. *Sci Rep*. 2021;11:11774.